

## RESEARCH ARTICLE

### Sources of marine carbonyl sulfide and its precursors traced by sulfur isotopes

Chen Davidson  <sup>1</sup>, Alon Angert, <sup>1\*</sup> Yasmin Avidani, <sup>1</sup> Sinikka T. Lennartz, <sup>2</sup> Marc von Hobe, <sup>3</sup> Alon Amrani  <sup>1\*</sup>

<sup>1</sup>The Institute of Earth Sciences, The Hebrew University of Jerusalem, Jerusalem, Israel; <sup>2</sup>Institute of Chemistry and Biology of the Marine Environment, Carl-von-Ossietzky Universität Oldenburg, Oldenburg, Germany; <sup>3</sup>Forschungszentrum Jülich GmbH, Institute of Climate and Energy Systems: Stratosphere (ICE-4), Jülich, Germany

#### Abstract

Carbonyl sulfide (OCS) is a major precursor of stratospheric sulfate aerosols and a proxy for terrestrial photosynthesis. In recent years, sulfur-isotope measurements ( $\delta^{34}\text{S}$ ) of OCS emerged as an approach to constrain the OCS budget. Yet, such measurements are still scarce for aquatic OCS. Here we present a large dataset of  $\delta^{34}\text{S}$  values of marine OCS. In addition, we present  $\delta^{34}\text{S}$  values of marine carbon disulfide (CS<sub>2</sub>) and dimethyl sulfide (DMS), which in the air, act as important precursors of tropospheric OCS. Samples were collected at the Atlantic Ocean, the Red Sea, the Mediterranean Sea, the Wadden Sea, and the North Sea. The gases were sampled by a water-air equilibrator, preserved in canisters, and analyzed via a preconcentration system coupled to a gas chromatograph connected to a multi-collector inductively coupled plasma mass spectrometer. We found  $\delta^{34}\text{S}$  values of  $-3.8\text{\textperthousand}$  to  $19.4\text{\textperthousand}$  for OCS,  $-10.5\text{\textperthousand}$  to  $20\text{\textperthousand}$  for CS<sub>2</sub>, and  $14\text{--}23\text{\textperthousand}$  for DMS. These  $\delta^{34}\text{S}$  values are controlled mainly by two endmembers: production in the water column and production in sediments. Lab experiments suggest that the  $^{34}\text{S}$ -fractionation of OCS photo-production is  $0.8\text{\textperthousand} \pm 0.5\text{\textperthousand}$ . In addition, based on measurements from the Atlantic Ocean, we calculated the  $^{34}\text{S}$ -fractionation of OCS dark-production as  $-6\text{\textperthousand} \pm 2\text{\textperthousand}$ . This new data significantly improves our knowledge of the sulfur isotope distribution of marine OCS and helps identify its different sources, sinks, and production pathways.

Carbonyl sulfide (OCS) is the most abundant long-lived sulfur gas in the troposphere, with a lifetime of a few years (Chin 1992). Tropospheric OCS acts as an important precursor for stratospheric sulfate aerosols, which increase Earth's albedo (Crutzen 1976; Hanson et al. 1994; Nagori et al. 2022). In the last two decades, OCS has been used as a proxy for terrestrial gross primary production, which controls atmospheric CO<sub>2</sub> concentration and regulates the Earth's climate (Montzka et al. 2007; Campbell et al. 2017; Lai et al. 2024). Tropospheric OCS is also used as a proxy for plants' stomatal conductance,

which helps estimate the water fluxes over entire forest plots (Wehr et al. 2017).

Oceans are considered the largest natural source of OCS and emit OCS both directly and indirectly via atmospheric oxidation of dimethyl sulfide (DMS) and carbon disulfide (CS<sub>2</sub>) (Chin and Davis 1993; Barnes et al. 1994; Von Hobe et al. 2023). An additional pathway of OCS production via the photolysis of aqueous phase DMS was also found (Modiri Gharehveran and Shah 2018).

Estimates of the atmospheric OCS budget are usually based on limited measurements backed by modeling, which leads to large uncertainties associated with OCS sinks and sources (Berry et al. 2013; Campbell et al. 2017; Whelan et al. 2018). Previously, the ocean–atmosphere flux was suggested to be as large as  $800 \text{ Gg yr}^{-1}$  based on estimates of a large “missing source” in the tropical oceans (Berry et al. 2013; Kuai et al. 2015). However, more recent measurements and process models of oceanic OCS concentrations suggest a smaller oceanic source of less than  $300 \text{ Gg yr}^{-1}$  (Lennartz et al. 2017; Lennartz et al. 2021).

\*Correspondence: [alon.angert@mail.huji.ac.il](mailto:alon.angert@mail.huji.ac.il); [alon.amrani@mail.huji.ac.il](mailto:alon.amrani@mail.huji.ac.il)

This is an open access article under the terms of the [Creative Commons Attribution-NonCommercial-NoDerivs](#) License, which permits use and distribution in any medium, provided the original work is properly cited, the use is non-commercial and no modifications or adaptations are made.

Associate editor: Rafel Simó

Sulfur isotope measurements of OCS were suggested as a new approach to reduce OCS budget uncertainties in the atmosphere, using an isotopic mass balance (Angert et al. 2019; Hattori et al. 2020; Davidson et al. 2021). To use this approach effectively,  $\delta^{34}\text{S}$  values of OCS in seawater and its precursors are required. In addition,  $^{34}\text{S}$ -fractionations of the main production and destruction pathways of oceanic OCS are also needed.

For marine DMS and its precursor, dimethylsulfoniopropionate (DMSP), several studies have presented relatively large datasets of  $\delta^{34}\text{S}$  values (Oduro et al. 2012; Amrani et al. 2013; Osorio-Rodriguez et al. 2021). However, such measurements for OCS and  $\text{CS}_2$  are currently scarce. Only two studies reported  $\delta^{34}\text{S}$  values of OCS and  $\text{CS}_2$  in natural seawater, based on limited measurements from the Mediterranean Sea and the Red Sea, which are not representative of the open ocean (Davidson et al. 2021; Davidson et al. 2025).

In the open ocean, OCS and  $\text{CS}_2$  are produced by the degradation of dissolved organic sulfur (DOS) compounds, which is the sulfur-containing fraction of dissolved organic matter. Surface ocean DOS was recently found to have a quite uniform  $\delta^{34}\text{S}$  value of  $18.6\text{‰} \pm 0.6\text{‰}$  (Phillips et al. 2022). The degradation of DOS can form OCS and  $\text{CS}_2$  via two main pathways: photochemical and light-independent, referred to here as photo-production and dark-production (Flöck and Andreae 1996; Von Hobe et al. 2003; Lennartz et al. 2021).

Previous studies suggested several pathways for photo-production of OCS and  $\text{CS}_2$ , involving intermediate radicals that react with various types of organic sulfur precursors within the DOS pool (Pos et al. 1998; Modiri Gharehveran and Shah 2018; Li et al. 2021).

Dark-production of OCS was suggested to be related to bacterial processes (Flöck and Andreae 1996) or to a reaction of organic sulfur compounds with thiyl radicals that can be generated in the dark, through metal catalyzation (Flöck et al. 1997; Von Hobe et al. 2001; Modiri Gharehveran and Shah 2018).

In addition to the surface ocean, there are several reports of enhanced OCS and  $\text{CS}_2$  production near sea coasts, salt marshes, and estuaries that reflect possible sedimentary sources (Zhang et al. 1998; DeLaune et al. 2002; Xu et al. 2024). This enhanced production is related to hydrogen sulfide ( $\text{H}_2\text{S}/\text{HS}^-$ ), which is produced via microbial sulfate reduction in anoxic sediments (Cutter and Radford-Knoery 1993; DeLaune et al. 2002; Xu et al. 2024).

Microbial sulfate reduction produces  $\text{H}_2\text{S}$  with a large  $^{34}\text{S}$ -fractionation, in the range of  $-20\text{‰}$  to  $-75\text{‰}$  (Wortmann et al. 2001; Brunner and Bernasconi 2005; Canfield et al. 2010). In addition, porewater DOS from different sediments was measured previously in the range of  $-2.7\text{‰}$  to  $+2.9\text{‰}$  (Phillips et al. 2022; Ibrahim and Tremblay 2023). Thus, we expect that OCS and  $\text{CS}_2$  which are related to sediments, will result in  $^{34}\text{S}$ -depleted OCS and  $\text{CS}_2$ , similar to DMS (Sela-Adler et al. 2016) and other volatile organic sulfur compounds

(Oduro et al. 2013). Yet, direct  $\delta^{34}\text{S}$  measurements of such OCS and  $\text{CS}_2$  that are associated with sedimentary sources are currently unavailable.

The main sink of oceanic OCS is hydrolysis, which is temperature and pH-dependent (Elliott et al. 1989; Radford-Knoery and Cutter 1994; Cutter et al. 2004). Marine OCS hydrolysis was recently found to have a  $^{34}\text{S}$ -fractionation of  $-2.6\text{‰} \pm 0.3\text{‰}$  (Avidani et al. 2024). The ocean–atmosphere flux accounts for the main sink of oceanic  $\text{CS}_2$  and the second most important sink for oceanic OCS after hydrolysis (Elliott 1990).

Here, we assess the main sources, production pathways, and associated  $^{34}\text{S}$ -fractionations that control the sulfur isotope distribution of marine OCS. We apply a two-pronged approach combining photochemical experiments to determine the  $^{34}\text{S}$ -fractionation of OCS formation and a multi-location data set of  $\delta^{34}\text{S}$  measurements of OCS,  $\text{CS}_2$ , and DMS, including the first open ocean samples.

## Methods

### Study sites

Several research campaigns were conducted. Research cruises were conducted at the Atlantic Ocean, the Wadden Sea, the North Sea, and the Mediterranean Sea. Shoreline campaigns were conducted at the Red Sea and Mediterranean Sea, as detailed in Fig. 1, Supporting Information Text S1, and Supporting Information Table S1. In all research campaigns, discrete samples were taken for later analysis of sulfur isotopes of OCS,  $\text{CS}_2$ , and DMS, as detailed below. In most research cruises, continuous onboard OCS measurements were conducted (Supporting Information Text S2), and in one cruise, DMSP samples were taken for later analysis of sulfur isotopes, as detailed below. We assume that all samples were taken from within the mixed layer, as sampling was done in depths of 0.5–5 m for most sampling campaigns (Supporting Information Text S1). Sampling from slightly deeper water ( $\sim 11$  m) was done onboard RV Polarstern during the open ocean campaign (Supporting Information Text S1). Yet, in this campaign, all samples were taken during sailing; hence, the ship's motion had mixed the water.

### Sampling procedure

For discrete OCS,  $\text{CS}_2$ , and DMS samples, we used a 20-L poly(methyl methacrylate) water–air equilibrator as described elsewhere (Davidson et al. 2021; Davidson et al. 2025). The equilibrator works with a seawater flow of  $\sim 10\text{-L min}^{-1}$ . After a minimum of 1 h equilibration, the headspace air was transferred to a 5, 10, or 25-L sampling bag via a cold trap that was used to capture water vapor. Then, the equilibrated gas samples were transferred to 3-L Silitek-treated canisters (SilicoCan; Restek, PA, USA) for preservation of up to 4.5 months before analysis.

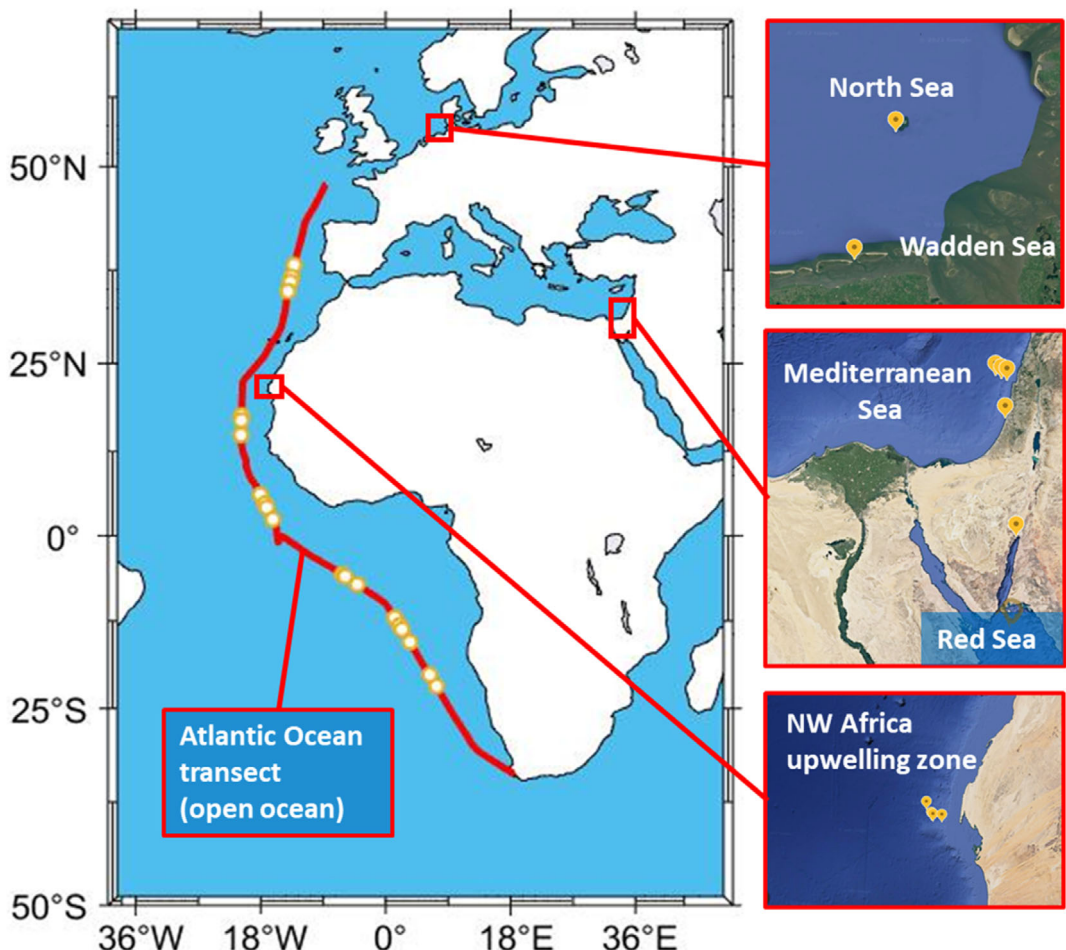


**Fig. 1.** Study sites: sampling locations at the Mediterranean Sea, the Red Sea, the Atlantic Ocean, the Wadden Sea, and the North Sea, detailed in Supporting Information Text S1 and Supporting Information Table S1.

For DMSP, we sampled seawater in 40 mL amber glass vials, covered with aluminum foil. For preservation of up to 1 yr, an HCl (37%) solution was added. For analysis, DMSP was converted to DMS using NaOH as detailed elsewhere (Amrani et al. 2013; Said-Ahmad and Amrani 2013). The  $\delta^{34}\text{S}$  values of DMSP in this paper are presented for total aqueous phase DMSP (dissolved and particulate).

### Sulfur isotope analysis

A description of the Materials and Standards used in this work is detailed in the Supporting Information Text S3. A pre-concentration system connected to a gas chromatograph (Trace 2000 series, Thermo, Germany) coupled with a Neptune Plus™ multi-collector inductively coupled plasma mass spectrometer (Thermo Scientific, Germany) was used, as described elsewhere (Angert et al. 2019; Davidson et al. 2021). The pre-concentration system is based on a Tenax resin trap (TA, 60–80 mesh; Sigma-Aldrich [MO, USA]), connected to a ten-port valve (Valco Instrument Co, TX, USA).

Our system demonstrates a precision of 6% (RSD) for concentrations and 0.6‰ for  $\delta^{34}\text{S}$  analysis of equilibrated gas samples from natural seawater, as detailed elsewhere (Davidson et al. 2025), and in the Supporting Information Text S4. A comparison of OCS concentrations measured on the multi-collector inductively coupled plasma mass spectrometer, vs. continuous OCS measurements (Supporting Information Text S4), excluding samples from the Wadden Sea, fits a linear regression with a slope of 0.92 ( $R^2 = 0.65$ ; Supporting Information Text S4; Supporting Information Fig. S2).

Two types of samples were introduced to the system, aqueous samples and equilibrated gas samples. Aqueous samples included total DMSP (both particulate and dissolved fractions [Del Valle et al. 2011]) from the Atlantic Ocean, and aqueous OCS and  $\text{CS}_2$  from photo-production experiments (Supporting Information Text S5). The aqueous samples were purged with helium and trapped on the preconcentration system, as detailed elsewhere (Said-Ahmad and Amrani 2013). Equilibrated gas samples from natural seawater, stored in 3-L canisters (see Sampling procedure), were connected to the

preconcentration system and pressurized with N<sub>2</sub>. The pressure in the canisters was then used to transfer the equilibrated gas samples from the canisters to the preconcentration system (Angert et al. 2019; Davidson et al. 2025).

After preconcentration, the samples were injected into the GC column (60 m × 0.320 mm, GS-GASPRO, Agilent Technologies, CA, USA) for the separation of sulfur compounds. The calibration gas standard (Supporting Information Text S3) was injected into the GC using a 100  $\mu$ L Sulfinert coated loop (Restek, PA, USA), connected to the 10-port valve. An additional six-port valve (Valco Instrument Co, TX, USA) was used to introduce SF<sub>6</sub> as an internal gas standard (Supporting Information Text S3). A transfer line, heated to 150°C, was used to transfer the samples from the GC to the plasma source (Said-Ahmad et al. 2017). The S species were atomized and ionized in the plasma source and yielded  $^{32}\text{S}^+$  and  $^{34}\text{S}^+$  ions that were transferred to the mass spectrometer unit for isotope ratio analysis.

Equilibrated gas samples (containing OCS, CS<sub>2</sub>, and DMS from natural seawater) were measured in the gas phase. To convert OCS, CS<sub>2</sub>, and DMS concentration from the gas phase to the aqueous phase, we used Henry's Law conversions. A temperature and salinity-dependent function was used for the OCS Henry constant (Ulshöfer et al. 1995), and a temperature-dependent Henry constant for DMS and CS<sub>2</sub> (Sander et al. 2006). The  $\delta^{34}\text{S}$  values of OCS, CS<sub>2</sub>, and DMS in this

study are presented as measured in the gas phase, which is representative of the  $\delta^{34}\text{S}$  values of the ocean-atmosphere flux. To convert the  $\delta^{34}\text{S}$  values from the gas phase to the aqueous phase, a  $^{34}\text{S}$ -fractionation during the aqueous-gas transition must be considered. Such fractionation was measured as  $0.6\text{‰} \pm 0.2\text{‰}$  for OCS (Davidson et al. 2025) and  $0.5\text{‰} \pm 0.2\text{‰}$  for DMS (Amrani et al. 2013). The  $^{34}\text{S}$ -fractionation during the aqueous-gas transition of CS<sub>2</sub> is currently unknown.

## Results

### Large range of $\delta^{34}\text{S}$ values for oceanic OCS and CS<sub>2</sub>

Presented here is a data set of sulfur isotope measurements of marine OCS and its precursors, CS<sub>2</sub> and DMS (Fig. 2). The concentrations of marine OCS from all of our sampling campaigns ranged from 2 to 243 pM, and OCS  $\delta^{34}\text{S}$  values ranged from  $-3.8\text{‰}$  to  $+19.4\text{‰}$  (Fig. 2a; Supporting Information Table S2). The concentrations of CS<sub>2</sub> ranged from 8 to 176 pM, and CS<sub>2</sub>  $\delta^{34}\text{S}$  values ranged from  $-10.5\text{‰}$  to  $+20\text{‰}$  (Fig. 2b; Supporting Information Table S2).

Dimethyl sulfide from our campaigns showed variable concentrations in the range of 0.2 to 30.5 nM (Fig. 2c; Supporting Information Table S2). Yet,  $\delta^{34}\text{S}$  values of DMS showed a much narrower range (14–23‰) than OCS and CS<sub>2</sub>.

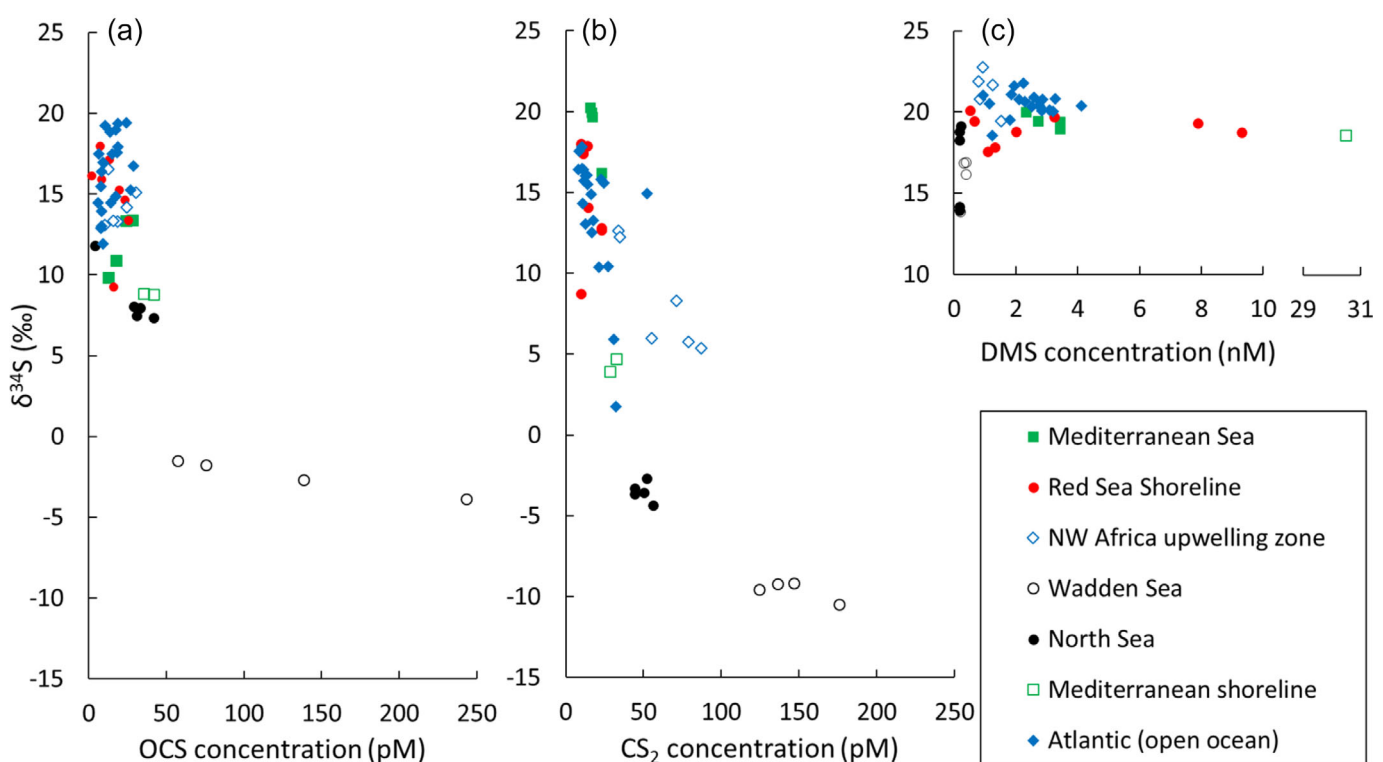


**Fig. 2.** Concentrations and  $\delta^{34}\text{S}$  values of the main volatile sulfur compounds in different marine and oceanic basins: (a) carbonyl sulfide (OCS), (b) carbon disulfide (CS<sub>2</sub>), and (c) dimethyl sulfide (DMS).

Furthermore, excluding the Wadden and North Seas, DMS shows a relatively uniform  $\delta^{34}\text{S}$  value of  $20\text{\textperthousand} \pm 1\text{\textperthousand}$  (Fig. 2c; Supporting Information Table S2). The DMS samples from the Wadden and North Seas had low DMS concentrations ( $\leq 0.4 \text{ nM}$ ) combined with interference from the water peak, which resulted in a larger analytical error for DMS  $\delta^{34}\text{S}$  values that can exceed  $1\text{\textperthousand}$ .

Total DMSP was sampled only during the Atlantic open ocean campaign. The DMSP concentrations in the Atlantic Ocean were in the range of  $10.3\text{--}77.4 \text{ nM}$ , yet their  $\delta^{34}\text{S}$  values were almost uniform at  $19.6\text{\textperthousand} \pm 0.5\text{\textperthousand}$  (Supporting Information Table S3; Supporting Information Fig. S2). The relatively uniform values of marine DMS and DMSP, presented here, are close to previously reported values of  $18\text{--}21\text{\textperthousand}$  for DMS and DMSP in surface marine water (Oduro et al. 2012; Amrani et al. 2013; Carnat et al. 2018).

In contrast to the uniform  $\delta^{34}\text{S}$  values of DMS/DMSP, the  $\delta^{34}\text{S}$  values of OCS and  $\text{CS}_2$  show a much larger variability at surface seawater across different basins (Fig. 2). Moreover, the  $\delta^{34}\text{S}$  values of OCS and  $\text{CS}_2$  from all marine environments, measured in the present study, were found to be correlated ( $R^2 = 0.68$ ; Fig. 3a). However, a much weaker correlation was found for  $\delta^{34}\text{S}$  values of OCS vs. DMS ( $R^2 = 0.40$ ; Fig. 3b).

#### Open ocean carbonyl sulfide shows diurnal cycles

The sulfur isotope values of OCS from the Atlantic open ocean showed the most  $^{34}\text{S}$ -enriched OCS among our different sampling campaigns, with a mean  $\delta^{34}\text{S}$  value of  $17\text{\textperthousand} \pm 2\text{\textperthousand}$  (Fig. 2a; Supporting Information Table S2). Samples of OCS

from the open ocean showed pronounced diurnal cycles in concentrations and  $\delta^{34}\text{S}$  values for most sampling days (Fig. 4). As opposed to OCS, the concentrations and  $\delta^{34}\text{S}$  values of  $\text{CS}_2$  and DMS from the same samples did not show diurnal cycles (Supporting Information Fig. S3).

A comparison between OCS samples taken during the afternoon and samples taken during dawn indicates two distinct groups ( $p\text{-value} \leq 0.05$ ). Where OCS that was sampled during dawn ( $n = 9$ ) showed a mean concentration of  $8 \pm 1 \text{ pM}$  and  $\delta^{34}\text{S}$  value of  $15\text{\textperthousand} \pm 2\text{\textperthousand}$ , while OCS samples taken during the afternoon ( $n = 6$ ) showed concentrations of  $20 \pm 5 \text{ pM}$  and OCS  $\delta^{34}\text{S}$  values of  $18\text{\textperthousand} \pm 1\text{\textperthousand}$  (Fig. 5).

#### Wadden Sea has $^{34}\text{S}$ -depleted volatile sulfur compounds

Our samples from the Wadden Sea, representing sediments-associated environments (see Supporting Information Text S1), show much higher OCS and  $\text{CS}_2$  concentrations (by an order of magnitude) compared with all other sampling campaigns (Fig. 2; Supporting Information Table S2). In addition, the  $\delta^{34}\text{S}$  values of OCS and  $\text{CS}_2$  from the Wadden Sea were  $^{34}\text{S}$ -depleted by  $15\text{--}25\text{\textperthousand}$ , compared with all other sampling campaigns (Fig. 2). Moreover,  $\delta^{34}\text{S}$  values of DMS from the Wadden Sea ( $16\text{\textperthousand} \pm 2\text{\textperthousand}$ ) were  $^{34}\text{S}$ -depleted by  $\sim 4\text{\textperthousand}$ , compared with  $\delta^{34}\text{S}$  values of DMS from most sampling campaigns ( $20\text{\textperthousand} \pm 1\text{\textperthousand}$  excluding the Wadden and North Seas). Similarly, in other environments with sediment inputs, a  $^{34}\text{S}$ -depleted DMS was previously reported (Sela-Adler et al. 2016).

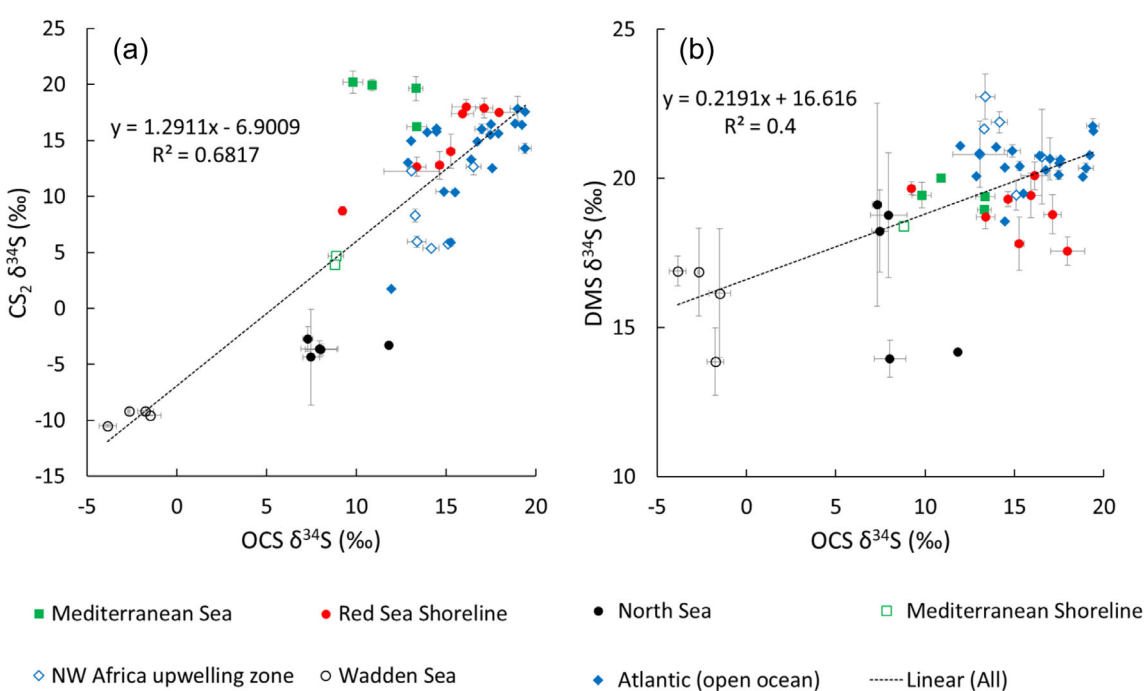


**Fig. 3.** Sulfur isotope values ( $\delta^{34}\text{S}$ ) of: (a) carbon disulfide ( $\text{CS}_2$ ) vs. carbonyl sulfide (OCS), (b) dimethyl sulfide (DMS) vs. OCS.

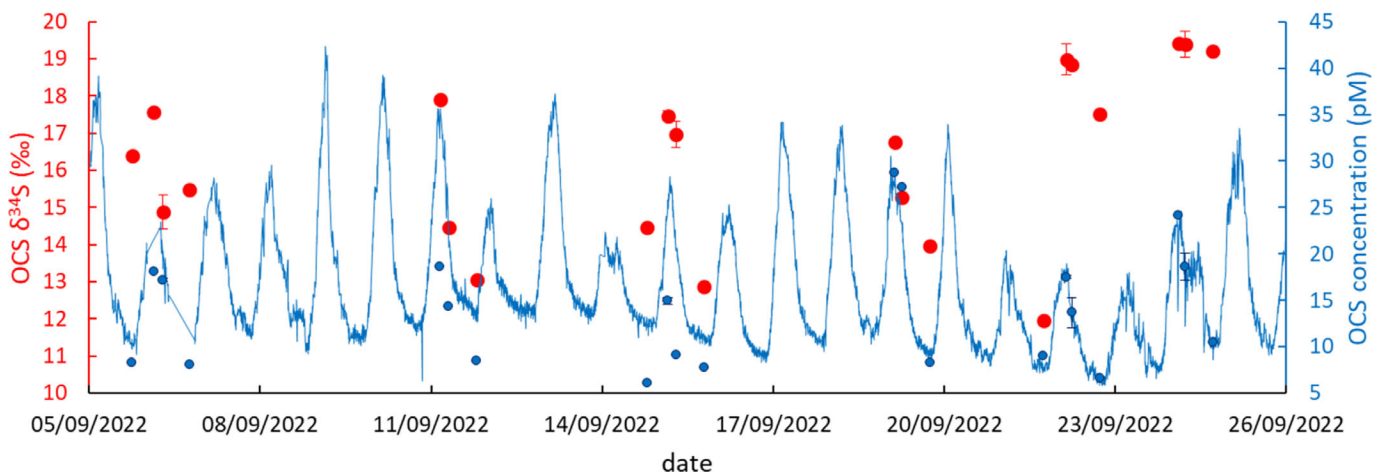


**Fig. 4.** Carbonyl sulfide (OCS) concentrations and sulfur isotopes from the Atlantic open ocean. Continuous onboard measurements of OCS concentration (blue line; pM), discrete measurements of OCS concentrations (blue circles; pM), and  $\delta^{34}\text{S}$  values (red circles; ‰). Error bars represent the standard deviation ( $1\sigma$ ) for OCS concentration and  $\delta^{34}\text{S}$  values of duplicate samples.

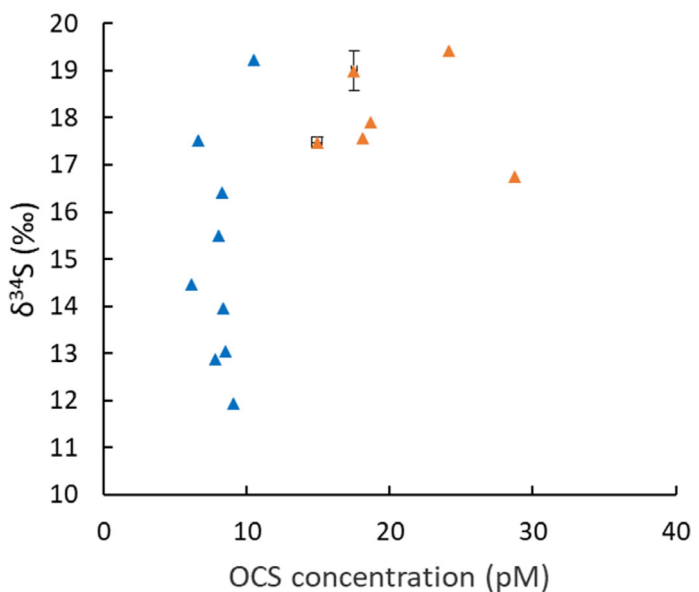


**Fig. 5.** Atlantic open ocean  $\delta^{34}\text{S}$  values of carbonyl sulfide (OCS) vs. its concentrations. The samples taken during dawn (blue triangles) and the samples taken during the afternoon (orange triangles) have distinct concentrations and  $\delta^{34}\text{S}$  values ( $p\text{-value} \leq 0.05$ ). The samples taken during dawn show a mean concentration of  $8 \pm 1$  pM and  $\delta^{34}\text{S}$  value of  $15\text{‰} \pm 2\text{‰}$  ( $n = 9$ ). The samples taken during the afternoon show higher concentrations of  $20 \pm 5$  pM and higher  $\delta^{34}\text{S}$  values of  $18\text{‰} \pm 1\text{‰}$  ( $n = 6$ ).

#### Wadden Sea carbonyl sulfides diurnal cycle

Samples of OCS from the Wadden Sea showed a pronounced diurnal cycle (Fig. 6), yet CS<sub>2</sub> and DMS showed a much weaker correlation to such a diurnal cycle (Supporting Information Fig. S3). The diurnal cycle of OCS in the Wadden Sea showed an opposite trend in  $\delta^{34}\text{S}$  values compared with the open ocean: In the Wadden Sea, OCS  $\delta^{34}\text{S}$  values showed a negative peak during maximum OCS concentration (Fig. 6).

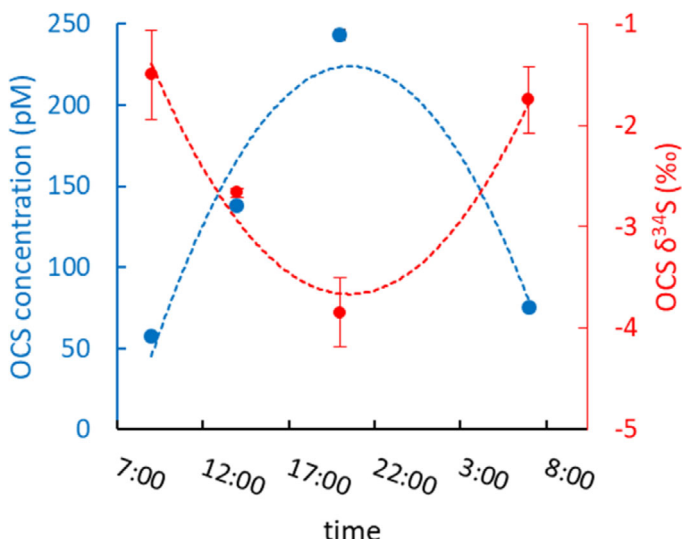


**Fig. 6.** Diurnal cycle of carbonyl sulfide (OCS) concentrations (blue) and  $\delta^{34}\text{S}$  values (red) in the Wadden Sea. The trendlines are fitted to second-order polynomial equations:  $y = -768.48x^2 + 7 \times 10^7x - 2 \times 10^{12}$  for concentrations ( $R^2 = 0.93$ ) and  $y = 9.8928x^2 - 87,996x + 2 \times 10^{10}$  for  $\delta^{34}\text{S}$  values ( $R^2 = 0.96$ ).

while in the open ocean, OCS  $\delta^{34}\text{S}$  values showed a positive peak during maximum OCS concentration (Fig. 4).

#### Steady state of carbonyl sulfide during photo-production experiments

For convenience, we use here  $\Delta^{34}\text{S}$  (‰) values, which are defined as the difference between the  $\delta^{34}\text{S}$  values of the products and the source (cysteine) according to Eq. 1.

$$\Delta^{34}\text{S} = \delta^{34}\text{S}_{\text{OCS}} - \delta^{34}\text{S}_{\text{cysteine}} \quad (1)$$

where  $\delta^{34}\text{S}_{\text{OCS}}$  is the measured  $\delta^{34}\text{S}$  value of carbonyl sulfide (OCS), or carbon disulfide ( $\text{CS}_2$ ) in the vial, and  $\delta^{34}\text{S}_{\text{cysteine}}$  is the  $\delta^{34}\text{S}$  value of the precursor, cysteine ( $3.8\text{‰} \pm 0.2\text{‰}$ ; Supporting Information Text S5).

All the data from the photo-production experiment presented here (OCS and  $\text{CS}_2$  concentrations and  $\Delta^{34}\text{S}$  values) are corrected for a “non-photochemical background” that was calculated based on dark and photo control experiments (see Supporting Information Tables S4, S5; Supporting Information Text S6). For information on dark-production experiments, see Supporting Information Text S7. Along the photo-production experiment, OCS concentration increased linearly up to 2.0 nM after 16 h (at a rate of  $0.125 \text{ nM h}^{-1}$ ) and then, toward the end of the experiment ( $\sim 29$  h), continued to increase at a much slower rate ( $0.03 \text{ nM h}^{-1}$ ) up to 2.4 nM (Fig. 7a; Supporting Information Table S5). The  $\Delta^{34}\text{S}$  values of OCS increased to a value of  $3.4\text{‰} \pm 0.5\text{‰}$  and remained stable after 16 h until the end of the experiment (Fig. 7a; Supporting Information Table S5).

The concentrations of  $\text{CS}_2$  increased exponentially throughout the experiment and reached a concentration of 0.7 nM after  $\sim 29$  h (Fig. 7b; Supporting Information Table S5). The  $\Delta^{34}\text{S}$  values of  $\text{CS}_2$  showed an abrupt increase to  $8.9\text{‰}$  in the first 18 h and then an abrupt decrease to  $3.8\text{‰}$  after  $\sim 29$  h (Fig. 7b; Supporting Information Table S6).

## Discussion

### Small isotopic fractionation during carbonyl sulfide photo-production

The photo-production experiment was aimed at calculating a first approximation of the effective  $^{34}\text{S}$ -fractionation during the photo-production of OCS and  $\text{CS}_2$ . To calculate this for OCS, one must consider the isotopic effect of the simultaneous OCS hydrolysis. This hydrolysis is a first-order

reaction, with a rate that depends on temperature and pH (Elliott et al. 1989). A recent study found that OCS hydrolysis has a  $^{34}\text{S}$  isotope fractionation of  $-2.6\text{‰} \pm 0.3\text{‰}$  between temperatures of  $4\text{--}22^\circ\text{C}$  (Avidani et al. 2024). Assuming there are no other significant production and destruction pathways, the OCS photo-production and OCS destruction via hydrolysis should eventually reach a steady state (Eq. 2).

$$\frac{d[\text{OCS}]}{dt} = F_{\text{photo}} - F_{\text{hydro}} = 0 \quad (2)$$

where  $[\text{OCS}]$  is carbonyl sulfide (OCS) concentration,  $F_{\text{photo}}$  is the flux of OCS photo-production,  $F_{\text{hydro}}$  is the flux of OCS hydrolysis. In our experiment, the OCS reached conditions that are close to a steady state after 16 h (Fig. 7a). To calculate the S isotope fractionation during OCS photo-production ( $\epsilon_{\text{photo}}$ ), assuming such a steady state (Eq. 2), we created an isotopic flux mass balance by multiplying each flux with its isotopic signature (Eq. 3).

$$F_{\text{photo}} * (\delta^{34}\text{S}_{\text{cysteine}} + \epsilon_{\text{photo}}) - F_{\text{hydro}} * (\delta^{34}\text{S}_{\text{OCS}} + \epsilon_{\text{hydro}}) = 0 \quad (3)$$

We then combined Eqs. 2 and 3, resulting in Eq. 4.

$$\epsilon_{\text{photo}} = \delta^{34}\text{S}_{\text{OCS}} + \epsilon_{\text{hydro}} - \delta^{34}\text{S}_{\text{cysteine}} \quad (4)$$

where  $\epsilon_{\text{photo}}$  is the  $^{34}\text{S}$ -fractionation associated with carbonyl sulfide (OCS) photo-production from cysteine,  $\delta^{34}\text{S}_{\text{OCS}}$  is the OCS isotopic value at steady state (after 16 h),  $\epsilon_{\text{hydro}}$  is the  $^{34}\text{S}$ -fractionation associated with OCS hydrolysis at  $4\text{--}22^\circ\text{C}$  ( $-2.6\text{‰}$ ; after Avidani et al. 2024), and  $\delta^{34}\text{S}_{\text{cysteine}}$  is the  $\delta^{34}\text{S}$  value of the precursor, cysteine ( $3.8\text{‰} \pm 0.2\text{‰}$ ; Supporting Information Text S5).

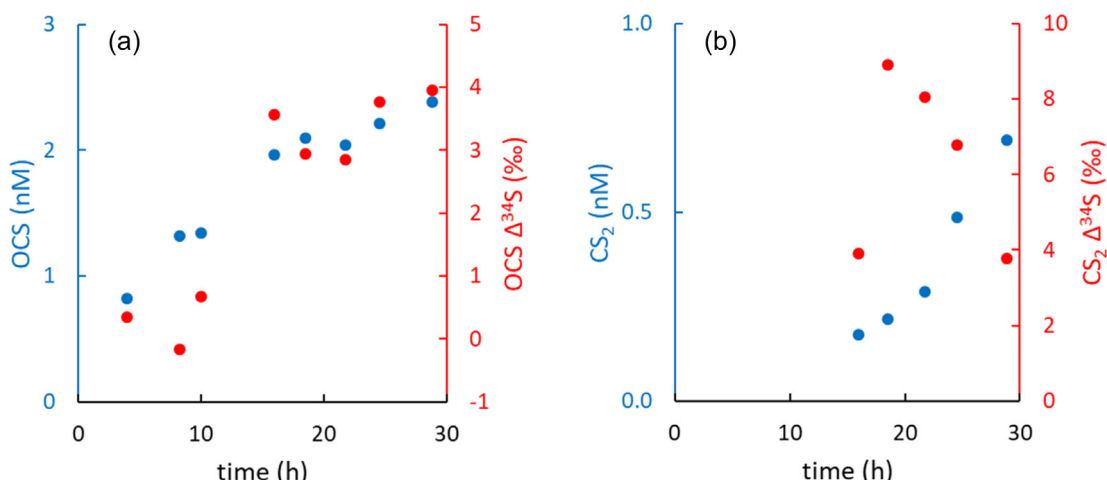


**Fig. 7.** Results of the photo-production experiment. Presented are the concentrations (nM) and the  $\Delta^{34}\text{S}$  values (‰) of the evolving products: (a) carbonyl sulfide (OCS) and (b) carbon disulfide ( $\text{CS}_2$ ). The  $\Delta^{34}\text{S}$  values are the difference between the  $\delta^{34}\text{S}$  values of the products (OCS or  $\text{CS}_2$ ) and the precursor, cysteine (Eq. 1).

Based on Eq. 4, we calculated the  $^{34}\text{S}$ -fractionation associated with OCS photo-production from cysteine ( $\epsilon_{\text{photo}}$ ) to be positive and small, with a value of  $+0.8\text{\textperthousand} \pm 0.5\text{\textperthousand}$ . A negative fractionation is usually the case for kinetic processes. However, a multi-step pathway, which involves several internal fractionations, may result in an overall positive apparent fractionation. Such a multi-step pathway is expected, as the photo-production of OCS is thought to be indirect, involving intermediate radicals (Pos et al. 1998; Modiri Gharehveran and Shah 2018; Li et al. 2021).

An important caveat in our experiment is that we used only cysteine as a precursor, which may not represent the large diversity of organosulfur precursors in natural seawater DOS. Nevertheless, photochemical studies of OCS formation have suggested that different organic sulfur precursors may have similar photochemical pathways (Modiri Gharehveran and Shah 2018). Hence, our calculated fractionation for OCS photo-production from cysteine ( $0.8\text{\textperthousand} \pm 0.5\text{\textperthousand}$ ) can be used as a first approximation.

As for the  $\text{CS}_2$ , measured in our photo-production experiment, the large increase followed by a large decrease in  $\Delta^{34}\text{S}$  values is difficult to explain by the fractionation of photo-production alone. While  $\text{CS}_2$  hydrolysis is assumed to be negligible for the removal of  $\text{CS}_2$  in surface water (Elliott 1990),  $\text{CS}_2$  destruction by photolysis is substantial (Lennartz et al. 2024), yet, with unknown associated  $^{34}\text{S}$ -fractionation. Thus, at this stage, we cannot determine the effective  $^{34}\text{S}$ -fractionation associated with the photo-production of  $\text{CS}_2$ .

### Similar $^{34}\text{S}$ for carbonyl sulfide and dissolved organic sulfur in open ocean

The OCS samples from the Atlantic open ocean showed a mean  $^{34}\text{S}$  value of  $17\text{\textperthousand} \pm 2\text{\textperthousand}$  (Fig. 2a; Supporting Information Table S2) with relatively stable  $^{34}\text{S}$  values over a vast area, between latitudes  $34^\circ\text{N}$  to  $22^\circ\text{S}$ . Furthermore, these samples show the most  $^{34}\text{S}$ -enriched OCS among our different sampling campaigns, which may indicate a negligible contribution of sediment-associated OCS (see Discussion). Thus, we suggest that the OCS  $^{34}\text{S}$  values from the Atlantic open ocean sampling campaign can be used as representatives for open oceans worldwide.

The  $17\text{\textperthousand} \pm 2\text{\textperthousand}$  value measured for open ocean OCS is close to the  $^{34}\text{S}$  value of its precursor, open ocean DOS in surface water ( $+18.6\text{\textperthousand} \pm 0.6\text{\textperthousand}$ ; after Phillips et al. 2022). We measured OCS in the gas phase, but DOS is found in the aqueous phase. Hence, the  $+0.6\text{\textperthousand} \pm 0.2\text{\textperthousand}$   $^{34}\text{S}$ -fractionation during the aqueous gas transition must be considered (Davidson et al. 2025), as detailed in Eq. 5.

$$\delta^{34}\text{S}_{\text{OCS}(\text{aq})} = \delta^{34}\text{S}_{\text{OCS}(\text{gas})} + \epsilon_{\text{aq-gas}} \quad (5)$$

where  $\delta^{34}\text{S}_{\text{OCS}(\text{aq})}$  is the  $^{34}\text{S}$  value of carbonyl sulfide (OCS) in the aqueous phase,  $\delta^{34}\text{S}_{\text{OCS}(\text{gas})}$  is the  $^{34}\text{S}$  value of OCS in the

gas phase, and  $\epsilon_{\text{aq-gas}}$  is the S isotope fractionation associated with the OCS aqueous-gas transition.

Considering the  $^{34}\text{S}$ -fractionation during the aqueous-gas transition brings the  $\delta^{34}\text{S}$  value of OCS and DOS in the open ocean even closer. Thus, the  $^{34}\text{S}$ -fractionations during OCS formation from DOS in the open ocean seem small. This is in agreement with our photo-production experiment, which found a small isotopic fractionation.

### Diurnal cycles of carbonyl sulfide in the open ocean

Pronounced diurnal cycles were found for OCS concentrations and  $\delta^{34}\text{S}$  values in the open ocean, and can be used to gain additional knowledge of OCS formation. During the afternoon, OCS is mostly controlled by daytime photo-production. Thus, we assume that the  $\delta^{34}\text{S}$  values of OCS in the afternoon are mostly controlled by the  $\delta^{34}\text{S}$  value of the OCS precursor (DOS) and the  $^{34}\text{S}$ -fractionation associated with OCS photo-production as detailed in Eq. 6.

$$\delta^{34}\text{S}_{\text{OCS}(\text{afternoon})} = \delta^{34}\text{S}_{\text{DOS}} + \epsilon_{\text{photo}} \quad (6)$$

where  $\delta^{34}\text{S}_{\text{OCS}(\text{afternoon})}$  is the mean  $^{34}\text{S}$  value of carbonyl sulfide (OCS) samples taken from the open ocean during the afternoon and corrected for the aqueous phase (Eq. 5),  $\delta^{34}\text{S}_{\text{DOS}}$  is the  $^{34}\text{S}$  value of open ocean dissolved organic sulfur (DOS) at surface water, and  $\epsilon_{\text{photo}}$  is the S isotope fractionation associated with the photo-production of OCS.

Using Eq. 6, and the previously reported value of  $18.6\text{\textperthousand} \pm 0.6\text{\textperthousand}$  for open ocean DOS (Phillips et al. 2022), we calculated an independent estimate of the sulfur isotope fractionation during the photo-production of OCS ( $\epsilon_{\text{photo}}$ ) as  $0\text{\textperthousand} \pm 1\text{\textperthousand}$ . The calculated  $\epsilon_{\text{photo}}$  (based on Eq. 6) and the lab-measured  $\epsilon_{\text{photo}}$  ( $0.8\text{\textperthousand} \pm 0.5\text{\textperthousand}$ ) for OCS photo-production from cysteine (see Photo-production experiments) have a similar value. This similarity increases our confidence that cysteine can be used as a representative model compound for OCS precursors in natural seawater DOS.

### Dark-production of carbonyl sulfide in the open ocean

During the nighttime, when no photo-production occurs, OCS concentration decreases until it reaches a minimum concentration before dawn. Assuming vertical transport within the mixed layer may be neglected (Von Hobe et al. 2003; Lennartz et al. 2019), a steady state between dark production and hydrolysis can be assumed at this time of day (Lennartz et al. 2017; Von Hobe et al. 2001), as shown in Eq. 7.

$$\frac{d[\text{OCS}]_{\text{dawn}}}{dt} = F_{\text{dark}} - F_{\text{hydro}} = 0 \quad (7)$$

where  $[\text{OCS}]_{\text{dawn}}$  is the mean carbonyl sulfide (OCS) concentration of samples taken from the open ocean during dawn,  $F_{\text{dark}}$  is the flux of OCS dark-production, and  $F_{\text{hydro}}$  is the flux of OCS destruction via hydrolysis.

The  $^{34}\text{S}$ -fractionation of OCS hydrolysis was recently measured as  $-2.6\text{\textperthousand} \pm 0.3\text{\textperthousand}$  (Avidani et al. 2024), which causes the remaining OCS in the water to be  $^{34}\text{S}$ -enriched. Hence, qualitatively, the  $^{34}\text{S}$ -fractionation of OCS dark-production must be negative to explain the decrease in OCS  $\delta^{34}\text{S}$  values during nighttime (Figs. 4, 5). To calculate a first approximation of the  $^{34}\text{S}$ -fractionation during OCS dark-production, we multiply each flux in Eq. 7 by its isotopic signature to create an isotopic flux mass balance (Eq. 8).

$$F_{\text{dark}} * (\delta^{34}\text{S}_{\text{DOS}} + \varepsilon_{\text{dark}}) - F_{\text{hydro}} * (\delta^{34}\text{S}_{\text{OCS(dawn)}} + \varepsilon_{\text{hydro}}) = 0 \quad (8)$$

We then combine Eqs. 7 and 8 to create Eq. 9.

$$\varepsilon_{\text{dark}} = \delta^{34}\text{S}_{\text{OCS(dawn)}} - \delta^{34}\text{S}_{\text{DOS}} + \varepsilon_{\text{hydro}} \quad (9)$$

where  $\delta^{34}\text{S}_{\text{DOS}}$  is the  $^{34}\text{S}$  value of the open ocean dissolved organic sulfur (DOS) at surface water,  $\varepsilon_{\text{dark}}$  is the S isotope fractionation associated with the dark production of carbonyl sulfide (OCS),  $\delta^{34}\text{S}_{\text{OCS(dawn)}}$  is the mean  $^{34}\text{S}$  value of OCS samples taken from the open ocean during dawn and corrected for the aqueous phase (Eq. 7), and  $\varepsilon_{\text{hydro}}$  is the S isotope fractionation associated with OCS hydrolysis (Avidani et al. 2024).

Based on Eqs. 7–9, we calculated a first approximation of the  $^{34}\text{S}$ -fractionation during OCS dark-production ( $\varepsilon_{\text{dark}}$ ) as  $-6\text{\textperthousand} \pm 2\text{\textperthousand}$ . This is a distinct fractionation compared with the S isotope fractionation associated with OCS photo-production ( $\varepsilon_{\text{photo}} = 0.8\text{\textperthousand} \pm 0.5\text{\textperthousand}$ ; see Photo-production experiment). The mechanism controlling OCS dark-production is debated; it was suggested to be related to either bacterial processes (Flöck and Andreae 1996) or chemical reactions of organic sulfur compounds with thiyl radicals (Flöck et al. 1997; Von Hobe et al. 2001; Modiri Gharehveran and Shah 2018). Future work on OCS S isotope measurements from dark incubation experiments may be beneficial to resolve this debate, as chemical and biological-production pathways often have different S isotope fractionations.

### Sedimentary sulfurization in the Wadden Sea

Our samples from the Wadden Sea showed  $^{34}\text{S}$ -depleted values for OCS,  $\text{CS}_2$ , and DMS compared with all other sampling campaigns (Fig. 3). These  $^{34}\text{S}$ -depleted values suggest the contribution of sedimentary reduced sulfur species, such as  $\text{H}_2\text{S}$ ,  $\text{HS}^-$ , and  $\text{S}_n^{2-}$ , produced via microbial sulfate reduction. Indeed, previous work showed  $^{34}\text{S}$  values of porewater  $\text{H}_2\text{S}/\text{HS}^-$  in a tidal flat at the Wadden Sea to be in the range of  $-13\text{\textperthousand}$  to  $-21\text{\textperthousand}$  (Böttcher et al. 1998).

In anoxic marine sediments, the reaction of  $^{34}\text{S}$ -depleted  $\text{HS}^-/\text{S}_n^{2-}$  with organic compounds (abiotic sulfurization) can produce organic compounds with an associated  $^{34}\text{S}$ -fractionation of  $\sim 5\text{\textperthousand}$  (Amrani and Aizenshtat 2004; Amrani et al. 2008). Thus, assuming no other fractionations, the

formation of OCS and  $\text{CS}_2$  via sulfurization in the Wadden Sea sediments should theoretically produce OCS and  $\text{CS}_2$  with a  $\delta^{34}\text{S}$  of  $-16\text{\textperthousand}$  to  $-8\text{\textperthousand}$ .

Our measured  $\text{CS}_2$   $\delta^{34}\text{S}$  values from the Wadden Sea ( $-10.5\text{\textperthousand}$  to  $-9.2\text{\textperthousand}$ ) are in the range of the theoretical calculation of sulfurization products above. This indicates that the formation of  $\text{CS}_2$  via sulfurization in porewater and transport to the overlying water may be the main pathway of  $\text{CS}_2$  production in the Wadden Sea. However, such a pathway may not fully explain the  $\delta^{34}\text{S}$  values of OCS in these samples ( $-3.8\text{\textperthousand}$  to  $-1.5\text{\textperthousand}$ ), which are  $^{34}\text{S}$ -enriched by  $\sim 5\text{\textperthousand}$  to  $9\text{\textperthousand}$  compared with  $\text{CS}_2$ .

### Sedimentary and open-ocean sources in the Wadden Sea

The Wadden Sea is affected by a semi-diurnal tidal regime. During high tides, North Sea surface water flows into the Wadden Sea. During low tides, the water from the Wadden Sea and porewater from the surrounding flats drains through the tidal channels back to the North Sea. Therefore, it is possible that the measured  $\delta^{34}\text{S}$  values of OCS at the Wadden Sea are affected by the mixing of two sources: 1. sediment-associated OCS (formed via sulfurization in porewater) and 2. “open ocean” OCS (formed via the photolysis of surface water DOS).

Assuming two endmembers (sediment-associated and open ocean), we used a keeling plot (Fig. 9) to calculate the  $^{34}\text{S}$  signatures of the sediment-associated endmember, where the  $\delta^{34}\text{S}$  value of the sediment-associated endmember is given by the y-intercept of the keeling plot. The OCS samples from the Wadden Sea show a good fit ( $R^2 = 0.90$ ) to the Keeling plot (Fig. 8), indicating a sediment-associated OCS endmember with a  $\delta^{34}\text{S}$  value of  $-4.2\text{\textperthousand} \pm 0.4\text{\textperthousand}$ . However,  $\text{CS}_2$  samples from the Wadden Sea show a much weaker correlation ( $R^2 = 0.47$ ) to the keeling plot, which may indicate that the two-endmembers assumption is not valid for  $\text{CS}_2$  at this sampling location. The relatively uniform  $\delta^{34}\text{S}$  values of  $\text{CS}_2$  in the Wadden Sea ( $-9.6\text{\textperthousand} \pm 0.6\text{\textperthousand}$ ) may indicate that  $\text{CS}_2$  at this location is almost entirely affected by sediment-associated production (sulfurization), with very little influence from the open ocean endmember.

The fact that OCS in the Wadden Sea seems to be affected by both endmembers, but  $\text{CS}_2$  produced mainly by sulfurization in the sediment may be related to the much lower photo-production rates of  $\text{CS}_2$  compared with OCS (Xie et al. 1998; Modiri Gharehveran and Shah 2018; Li et al. 2021). In addition, OCS in water is consumed rapidly by hydrolysis, within hours to days (Elliott et al. 1989). Hence, a considerable portion of the sulfurized OCS may be hydrolyzed before it diffuses from sediment porewater to the overlying water. The known removal processes of marine  $\text{CS}_2$  are mostly found at the sea surface (photolysis and degassing), whereas  $\text{CS}_2$  hydrolysis is assumed to be negligible (Elliott 1990; Lennartz et al. 2024). Hence, at the sediment–water interface,

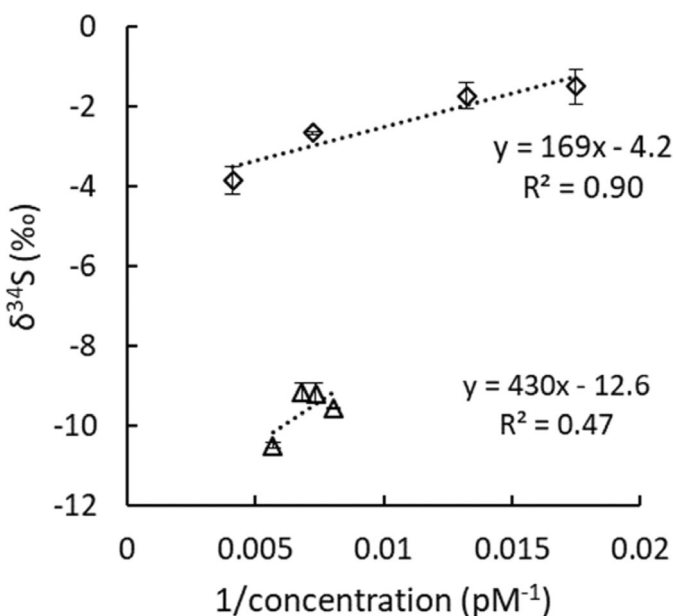


**Fig. 8.** Keeling plots for samples from the Wadden Sea. Carbonyl sulfide (OCS; black diamonds) show a good linear fit, indicating a sediment-associated OCS contribution with a  $\delta^{34}\text{S}$  value of  $-4.2\text{\textperthousand} \pm 0.4\text{\textperthousand}$ . Carbon disulfide (CS<sub>2</sub>; black triangles) show a weaker correlation, which may indicate that a two-endmember assumption is not valid. The error bars represent the standard variation (1 $\sigma$ ) for duplicates of OCS and CS<sub>2</sub>  $\delta^{34}\text{S}$  values.

CS<sub>2</sub> removal is negligible. Thus, a larger portion of the sulfurized CS<sub>2</sub> can reach from the sediment to the overlying water.

#### Photo-production of carbonyl sulfide from sedimentary precursors

An important difference between OCS and CS<sub>2</sub> in the Wadden Sea is related to their diurnal variability. A weak diurnal cycle was found for CS<sub>2</sub> (Supporting Information Fig. S3), which makes sense if indeed the main pathway of CS<sub>2</sub> production in the Wadden Sea is via the sulfurization in porewater and then transport to the overlying water. Such a pathway is not expected to be significantly affected by sunlight. However, OCS showed a pronounced, 24 h cycle with a negative  $\delta^{34}\text{S}$  value at its peak. We expected that during low tides, when porewater drains from the sediments to the tidal channel, OCS concentration would rise. However, it seems that there is no correlation between OCS and the ~12-h semidiurnal tides. Instead, the 24-h cycle of OCS in the Wadden Sea (Fig. 7), together with the keeling plot (Fig. 9), may indicate a different OCS production pathway.

We suggest a multi-step production pathway that starts with the diffusion of  $^{34}\text{S}$ -depleted sulfurized DOS from the sediment to the overlying water, which is then exposed to sunlight (photochemistry) and produces OCS with a  $\delta^{34}\text{S}$  value of  $-4.2\text{\textperthousand} \pm 0.4\text{\textperthousand}$ . This suggested pathway is distinct from the direct diffusion of sulfurized OCS from the sediment

to the water column or from the degradation of open ocean DOS (Fig. 9) and seems to better explain our results.

#### Dissolved organic sulfur transport affects the $\delta^{34}\text{S}$ of carbonyl sulfide

Our sampling location at the North Sea was only 50 km away from the sampling location at the Wadden Sea and 15–25 m above the seafloor. Thus, the contribution of sulfurized OCS, CS<sub>2</sub>, and DOS was possible by vertical transport from below the sediment and by lateral transport from the nearby Wadden Sea. Indeed, the samples from the North Sea (OCS  $\delta^{34}\text{S} = 8\text{\textperthousand} \pm 2\text{\textperthousand}$ ; CS<sub>2</sub>  $\delta^{34}\text{S} = -4\text{\textperthousand} \pm 2\text{\textperthousand}$ ) showed  $^{34}\text{S}$ -depleted values compared with the open ocean (OCS  $\delta^{34}\text{S} = 17\text{\textperthousand} \pm 2\text{\textperthousand}$ ; CS<sub>2</sub>  $\delta^{34}\text{S} = 14\text{\textperthousand} \pm 4\text{\textperthousand}$ ). This indicates that sedimentary-sourced OCS and CS<sub>2</sub> probably had reached our sampling location in the North Sea. Similarly, wave mixing effects in the Red Sea shoreline suggest that wave action may have an important role in releasing sedimentary-sourced OCS, CS<sub>2</sub>, or DOS in coastal regions (Supporting Information Text S8).

Our samples from the Mediterranean Sea and NW Africa upwelling zone showed slightly  $^{34}\text{S}$ -depleted OCS and CS<sub>2</sub> values compared with the open ocean (Fig. 2). However, the short-lived OCS is consumed by hydrolysis within a timescale of hours to days (Elliott et al. 1989), and the lifetime of CS<sub>2</sub> in the surface ocean is thought to be in the order of weeks (Elliott 1990). Thus, it is unlikely that sulfurized OCS and CS<sub>2</sub>, which are produced in sediments, will survive the transport to distant locations such as our sampling locations at the Mediterranean Sea and NW Africa upwelling zone (see Supporting Information Text S9).

As a precursor of OCS and CS<sub>2</sub>, the long-lived DOS (~4000 yr; after Ksionzek et al. 2016) can carry the distinct  $^{34}\text{S}$ -depleted signature of the sediments, via upwelling or lateral currents, to vast distances. Then, such  $^{34}\text{S}$ -depleted DOS can reach surface water, where it can produce OCS and CS<sub>2</sub> by photo-production (Supporting Information Text S9).

Similarly, terrestrial-sourced DOS from plant residues, which typically carries  $\delta^{34}\text{S}$  values of 0–8‰ (Peterson et al. 1985; Alling et al. 2008; Ibrahim and Tremblay 2023), can also be transported via river drainage and lateral ocean currents. A recent study suggested that terrestrial DOS runoff can significantly enhance OCS photo-production in the Bay of Bengal (Xu et al. 2024). We expect that such terrestrial-sourced DOS should produce  $^{34}\text{S}$ -depleted OCS and CS<sub>2</sub> in the surface ocean and may partially explain the natural variability in OCS and CS<sub>2</sub>  $\delta^{34}\text{S}$  values (Supporting Information Text S9).

On the global scale, sulfurized porewater DOS and terrestrial DOS account for a small component of oceanic DOS (Phillips et al. 2022; Ibrahim and Tremblay 2023). Nevertheless, due to the distinct  $^{34}\text{S}$ -depleted values of sulfurized porewater and terrestrial DOS, they may affect the  $\delta^{34}\text{S}$  value of oceanic DOS even at small concentrations. Thus, the transport and photolysis of such  $^{34}\text{S}$ -depleted DOS may partially

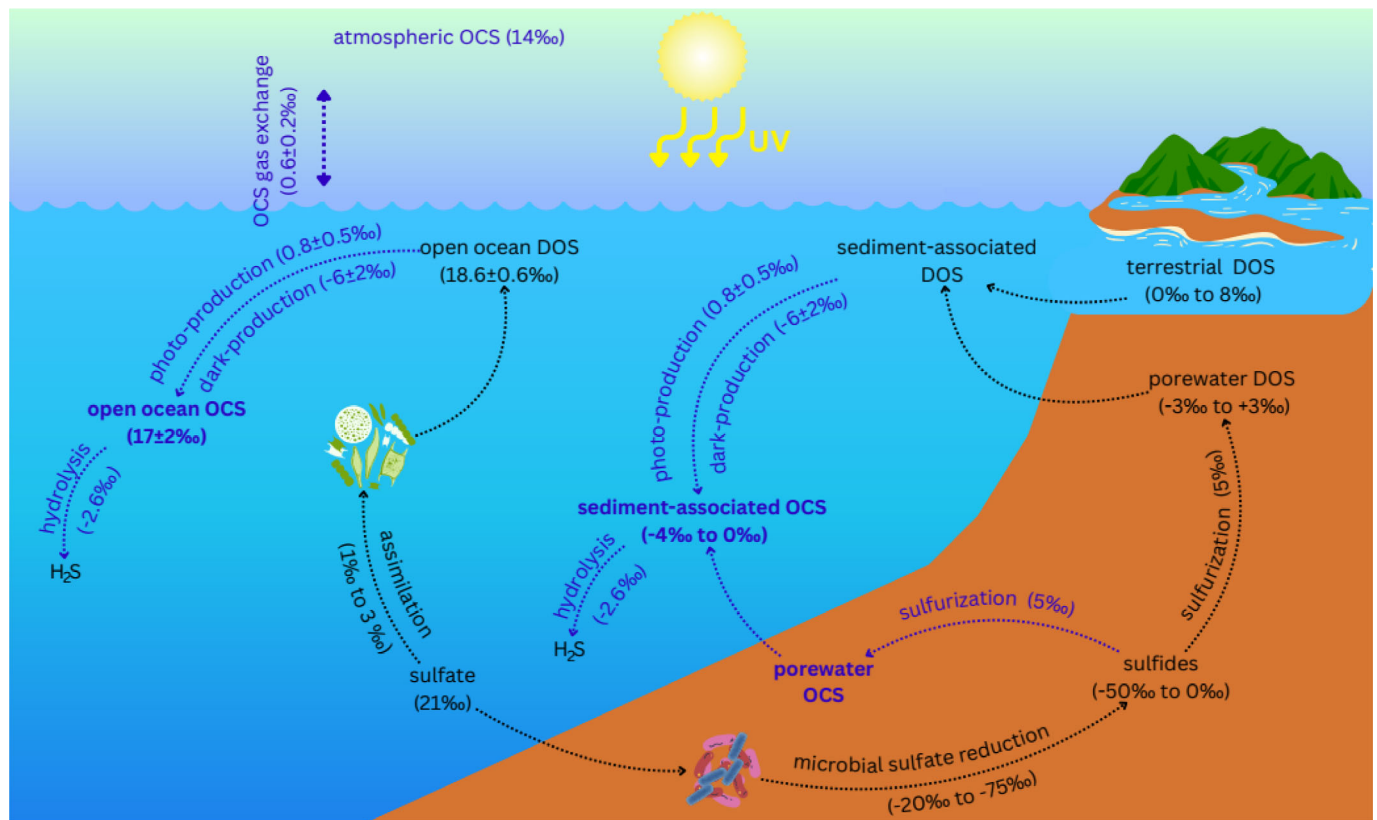


**Fig. 9.** Schematics of marine carbonyl sulfide (OCS) production and destruction pathways. The scheme present  $\delta^{34}\text{S}$  values of marine OCS and its main precursor, dissolved organic sulfur (DOS) from different sources and the associated  $^{34}\text{S}$ -fractionations related to major production and destruction pathways. Part of the  $\delta^{34}\text{S}$  values and  $^{34}\text{S}$ -fractionations presented here follow after other works as detailed: The  $\delta^{34}\text{S}$  value of atmospheric OCS after Davidson et al. (2025); The  $\delta^{34}\text{S}$  value of sulfate, after Kaplan and Rittenberg (1964); The  $\delta^{34}\text{S}$  values of porewater DOS, open ocean DOS, and terrestrial DOS after Phillips et al. (2022) and Ibrahim and Tremblay (2023); The  $^{34}\text{S}$ -fractionation during OCS hydrolysis, after Avidani et al. (2024); The  $^{34}\text{S}$ -fractionation during sulfurization, after Amrani and Aizenshtat (2004) and Amrani et al. (2008); The  $\delta^{34}\text{S}$  value of sulfides in sediments and the  $^{34}\text{S}$ -fractionation during microbial sulfate reduction, after Wortmann et al. (2001), Brunner and Bernasconi (2005), and Canfield et al. (2010).

explain the natural variability of  $\delta^{34}\text{S}$  values of OCS and  $\text{CS}_2$  observed in our campaigns.

## Conclusions

Large variability in the  $\delta^{34}\text{S}$  values of marine OCS and  $\text{CS}_2$  was recorded in different marine environments. In contrast, the  $\delta^{34}\text{S}$  values of DMS showed a narrower range across most sampling locations. This suggests different formation pathways of OCS and  $\text{CS}_2$  than those of DMS. We demonstrated that the spatial  $\delta^{34}\text{S}$  variability of OCS and  $\text{CS}_2$  is mainly affected by two endmembers: open ocean and sediments. Their proportional mixtures determine the  $\delta^{34}\text{S}$  values of OCS and  $\text{CS}_2$ . In addition, OCS  $\delta^{34}\text{S}$  value varies on a diurnal basis due to the different  $^{34}\text{S}$  fractionations of OCS associated with photo-production, dark-production, and hydrolysis. Fig. 9 summarizes the main production and destruction pathways of marine OCS and their associated  $^{34}\text{S}$  values and fractionations.

There is evidence that OCS in the Wadden Sea is mainly produced by the transport of  $^{34}\text{S}$ -depleted sulfurized DOS from

the sediment to surface water, followed by photolysis. Such sulfurized DOS may influence the  $\delta^{34}\text{S}$  values of OCS and  $\text{CS}_2$  at a lateral distance of tens of kilometers from estuaries or coastal sediments. A similar influence of such precursors may be associated with upwelling currents at even greater distances from shore ( $\sim 150$  km).

These results significantly improve our knowledge of the sulfur isotope distribution of marine OCS and help identify its different sources, sinks, and production pathways. This, in turn, can improve future models of the ocean-atmosphere OCS flux.

## Author Contributions

Chen Davidson: Methodology, collecting samples, validation, conceptualization, experiments, processing data, writing – original draft. Alon Angert: Methodology, validation, conceptualization, writing – review and editing, supervision. Yasmin Avidani: collecting and processing samples, analyses. Sinnika T. Lennartz: conceptualization, collecting samples,

analyses, writing – review and editing. Marc von Hobe: collecting samples, analyses, writing – review and editing. Alon Amrani: Methodology, validation, conceptualization, writing – review and editing, supervision.

## Acknowledgments

We thank Heike Simon for helping during sampling onboard RV Polarstern and RV Senckenberg, and Christa Marandino for providing sampling equipment. We thank Jack Silverman for arranging our sampling onboard the RV Bat-Galim. We also thank Tal Weiner for helping during sampling at the Mediterranean shoreline and the Red Sea. We appreciate the constructive comments by the two reviewers and the editors. The authors acknowledge funding from the Israeli Ministry of Science and Culture of Lower Saxony/Volkswagen Foundation “Niedersächsisches Vorab” for Grants VWZN3621 and 16TTP079, and funding from the Israel Science Foundation for grants 300/23 and 2086/23.

## Conflicts of Interest

None declared.

## Data Availability Statement

Data are available per request from the authors.

## References

Alling, V., C. Humborg, C.-M. Mörth, L. Rahm, and F. Pollehn. 2008. “Tracing Terrestrial Organic Matter by  $\delta^{34}\text{S}$  and  $\delta^{13}\text{C}$  Signatures in a Subarctic Estuary.” *Limnology and Oceanography* 53, no. 6: 2594–2602. <https://doi.org/10.4319/lo.2008.53.6.2594>.

Amrani, A., and Z. Aizenshtat. 2004. “Mechanisms of Sulfur Introduction Chemically Controlled:  $\delta^{34}\text{S}$  Imprint.” *Organic Geochemistry* 35, no. 11–12: 1319–1336. <https://doi.org/10.1016/j.orggeochem.2004.06.019>.

Amrani, A., Q. Ma, W. S. Ahmad, Z. Aizenshtat, and Y. Tang. 2008. “Sulfur Isotope Fractionation During Incorporation of Sulfur Nucleophiles Into Organic Compounds.” *Chemical Communications* 11: 1356–1358. <https://doi.org/10.1039/B717113G>.

Amrani, A., W. Said-Ahmad, Y. Shaked, and R. P. Kiene. 2013. “Sulfur Isotope Homogeneity of Oceanic DMSP and DMS.” *Proceedings of the National Academy of Sciences of the United States of America* 110, no. 46: 18413–18418. <https://doi.org/10.1073/pnas.1312956110>.

Angert, A., W. Said-Ahmad, C. Davidson, and A. Amrani. 2019. “Sulfur Isotopes Ratio of Atmospheric Carbonyl Sulfide Constrains Its Sources.” *Scientific Reports* 9, no. 1: 1–8. <https://doi.org/10.1038/s41598-018-37131-3>.

Avidani, Y., A. Angert, C. Davidson, X. Xia, Y. Gao, and A. Amrani. 2024. “Sulfur Isotopic Fractionation During Hydrolysis of Carbonyl Sulfide.” *Marine Chemistry* 267: 104458. <https://doi.org/10.1016/j.marchem.2024.104458>.

Barnes, I., K. Becker, and I. Patroescu. 1994. “The Tropospheric Oxidation of Dimethyl Sulfide: A New Source of Carbonyl Sulfide.” *Geophysical Research Letters* 21, no. 22: 2389–2392. <https://doi.org/10.1029/94GL02499>.

Berry, J., A. Wolf, J. E. Campbell, et al. 2013. “A Coupled Model of the Global Cycles of Carbonyl Sulfide and  $\text{CO}_2$ : A Possible New Window on the Carbon Cycle.” *Journal of Geophysical Research: Biogeosciences* 118, no. 2: 842–852. <https://doi.org/10.1002/jgrg.20068>.

Böttcher, M. E., B. Oelschläger, T. Höpner, H.-J. Brumsack, and J. Rullkötter. 1998. “Sulfate Reduction Related to the Early Diagenetic Degradation of Organic Matter and ‘Black Spot’ Formation in Tidal Sandflats of the German Wadden Sea (Southern North Sea): Stable Isotope ( $^{13}\text{C}$ ,  $^{34}\text{S}$ ,  $^{18}\text{O}$ ) and Other Geochemical Results.” *Organic Geochemistry* 29, no. 5–7: 1517–1530. [https://doi.org/10.1016/S0146-6380\(98\)00124-7](https://doi.org/10.1016/S0146-6380(98)00124-7).

Brunner, B., and S. M. Bernasconi. 2005. “A Revised Isotope Fractionation Model for Dissimilatory Sulfate Reduction in Sulfate Reducing Bacteria.” *Geochimica et Cosmochimica Acta* 69, no. 20: 4759–4771. <https://doi.org/10.1016/j.gca.2005.04.015>.

Campbell, J., J. Berry, U. Seibt, et al. 2017. “Large Historical Growth in Global Terrestrial Gross Primary Production.” *Nature* 544, no. 7648: 84–87. <https://doi.org/10.1038/nature22030>.

Canfield, D. E., J. Farquhar, and A. L. Zerkle. 2010. “High Isotope Fractionations during Sulfate Reduction in a Low-Sulfate Euxinic Ocean Analog.” *Geology* 38, no. 5: 415–418. <https://doi.org/10.1130/G30723.1>.

Carnat, G., W. Said-Ahmad, F. Fripiat, et al. 2018. “Variability in Sulfur Isotope Composition Suggests Unique Dimethylsulfoniopropionate Cycling and Microalgae Metabolism in Antarctic Sea Ice.” *Communications Biology* 1, no. 1: 1–9. <https://doi.org/10.1038/s42003-018-0228-y>.

Chin, M. 1992. “Atmospheric Studies of Carbonyl Sulfide and Carbon Disulfide and their Relationship to Stratospheric Background Sulfur Aerosol.” Doctoral Dissertation. Georgia Institute of Technology <https://doi.org/10.1136/bjsm.26.4.262>.

Chin, M., and D. D. Davis. 1993. “Global Sources and Sinks of OCS and CS<sub>2</sub> and Their Distributions.” *Global Biogeochemical Cycles* 7, no. 2: 321–337. <https://doi.org/10.1029/93GB00568>.

Crutzen, P. J. 1976. “The Possible Importance of CSO for the Sulfate Layer of the Stratosphere.” *Geophysical Research Letters* 3, no. 2: 73–76. <https://doi.org/10.1029/GL003i002p00073>.

Cutter, G. A., L. S. Cutter, and K. C. Filippino. 2004. “Sources and Cycling of Carbonyl Sulfide in the Sargasso Sea.” *Limnology and Oceanography* 49, no. 2: 555–565. <https://doi.org/10.4319/lo.2004.49.2.0555>.

Cutter, G. A., and J. Radford-Knoery. 1993. “Carbonyl Sulfide in Two Estuaries and Shelf Waters of the Western North Atlantic Ocean.” *Marine Chemistry* 43, no. 1–4: 225–233. [https://doi.org/10.1016/0304-4203\(93\)90228-G](https://doi.org/10.1016/0304-4203(93)90228-G).

Davidson, C., A. Amrani, and A. Angert. 2021. "Tropospheric Carbonyl Sulfide Mass Balance Based on Direct Measurements of Sulfur Isotopes." *Proceedings of the National Academy of Sciences of the United States of America* 118, no. 6: 1–6. <https://doi.org/10.1073/pnas.2020060118>.

Davidson, C., A. Angert, Y. Avidani, T. Weiner, and A. Amrani. 2025. "Sulfur Isotopes Analysis of Marine Carbonyl Sulfide and Its Precursors." SSRN <https://doi.org/10.2139/ssrn.5145889>.

Del Valle, D. A., D. Slezak, C. M. Smith, A. N. Rellinger, D. J. Kieber, and R. P. Kiene. 2011. "Effect of Acidification on Preservation of DMSP in Seawater and Phytoplankton Cultures: Evidence for Rapid Loss and Cleavage of DMSP in Samples Containing *Phaeocystis* Sp." *Marine Chemistry* 124, no. 1–4: 57–67. <https://doi.org/10.1016/j.marchem.2010.12.002>.

DeLaune, R., I. Devai, and C. Lindau. 2002. "Flux of Reduced Sulfur Gases Along a Salinity Gradient in Louisiana Coastal Marshes." *Estuarine, Coastal and Shelf Science* 54, no. 6: 1003–1011. <https://doi.org/10.1006/ecss.2001.0871>.

Elliott, S. 1990. "Effect of Hydrogen Peroxide on the Alkaline Hydrolysis of Carbon Disulfide." *Environmental Science & Technology* 24, no. 2: 264–267. <https://doi.org/10.1021/es00072a017>.

Elliott, S., E. Lu, and F. S. Rowland. 1989. "Rates and Mechanisms for the Hydrolysis of Carbonyl Sulfide in Natural Waters." *Environmental Science & Technology* 23, no. 4: 458–461. <https://doi.org/10.1021/es00181a011>.

Flöck, O. R., and M. O. Andreae. 1996. "Photochemical and Non-Photochemical Formation and Destruction of Carbonyl Sulfide and Methyl Mercaptan in Ocean Waters." *Marine Chemistry* 54, no. 1–2: 11–26. [https://doi.org/10.1016/0304-4203\(96\)00027-8](https://doi.org/10.1016/0304-4203(96)00027-8).

Flöck, O. R., M. O. Andreae, and M. Dräger. 1997. "Environmentally Relevant Precursors of Carbonyl Sulfide in Aquatic Systems." *Marine Chemistry* 59, no. 1–2: 71–85. [https://doi.org/10.1016/S0304-4203\(97\)00012-1](https://doi.org/10.1016/S0304-4203(97)00012-1).

Hanson, D. R., A. Ravishankara, and S. Solomon. 1994. "Heterogeneous Reactions in Sulfuric Acid Aerosols: A Framework for Model Calculations." *Journal of Geophysical Research-Atmospheres* 99, no. D2: 3615–3629. <https://doi.org/10.1029/93JD02932>.

Hattori, S., K. Kamezaki, and N. Yoshida. 2020. "Constraining the Atmospheric OCS Budget From Sulfur Isotopes." *Proceedings of the National Academy of Sciences* 117, no. 34: 20447–20452. <https://doi.org/10.1073/pnas.2007260117>.

Ibrahim, H., and L. Tremblay. 2023. "Origin of Dissolved Organic Sulfur in Marine Waters and the Impact of Abiotic Sulfurization on Its Composition and Fate." *Marine Chemistry* 254: 104273. <https://doi.org/10.1016/j.marchem.2023.104273>.

Kaplan, I., and S. Rittenberg. 1964. "Microbiological Fractionation of Sulphur Isotopes." *Microbiology* 34: 195–212.

Ksionzek, K. B., O. J. Lechtenfeld, S. L. McCallister, et al. 2016. "Dissolved Organic Sulfur in the Ocean: Biogeochemistry of a Petagram Inventory." *Science* 354, no. 6311: 456–459. <https://doi.org/10.1126/science.aaf7796>.

Kuai, L., J. R. Worden, J. E. Campbell, et al. 2015. "Estimate of Carbonyl Sulfide Tropical Oceanic Surface Fluxes Using Aura Tropospheric Emission Spectrometer Observations." *Journal of Geophysical Research: Atmospheres* 120, no. 20: 11012–11023. <https://doi.org/10.1002/2015JD023493>.

Lai, J., L. M. Kooijmans, W. Sun, et al. 2024. "Terrestrial Photosynthesis Inferred From Plant Carbonyl Sulfide Uptake." *Nature* 634: 6855–6861. <https://doi.org/10.1038/s41586-024-08050-3>.

Lennartz, S. T., M. Gauss, M. von Hobe, and C. A. Marandino. 2021. "Monthly Resolved Modelled Oceanic Emissions of Carbonyl Sulphide and Carbon Disulphide for the Period 2000–2019." *Earth System Science Data* 13, no. 5: 2095–2110. <https://doi.org/10.5194/essd-13-2095-2021>.

Lennartz, S. T., C. Marandino, M. von Hobe, et al. 2017. "Direct Oceanic Emissions Unlikely to Account for the Missing Source of Atmospheric Carbonyl Sulfide." *Atmospheric Chemistry and Physics* 17, no. 1: 385–402. <https://doi.org/10.5194/acp-17-385-2017>.

Lennartz, S. T., H. Simon, D. Booge, L. Zhou, and C. Marandino. 2024. "CS2 Cycling in Seawater: Dark Production and UV Light Driven Consumption." *Geophysical Research Letters* 51, no. 5: e2023GL107024. <https://doi.org/10.1029/2023GL107024>.

Lennartz, S., M. Von Hobe, D. Booge, et al. 2019. "The Influence of Dissolved Organic Matter on the Marine Production of Carbonyl Sulfide (OCS) and Carbon Disulfide (CS2) in the Peruvian Upwelling." *Ocean Science* 15: 1071–1090.

Li, J.-L., X. Zhai, and L. Du. 2021. "Photosensitized Formation of Sulfate and Volatile Sulfur Gases From Dissolved Organic Sulfur: Roles of pH, Dissolved Oxygen, and Salinity." *Science of the Total Environment* 786: 147449. <https://doi.org/10.1016/j.scitotenv.2021.147449>.

Modiri Gharehveran, M., and A. D. Shah. 2018. "Indirect Photochemical Formation of Carbonyl Sulfide and Carbon Disulfide in Natural Waters: Role of Organic Sulfur Precursors, Water Quality Constituents, and Temperature." *Environmental Science & Technology* 52, no. 16: 9108–9117. <https://doi.org/10.1021/acs.est.8b01618>.

Montzka, S., P. Calvert, B. Hall, et al. 2007. "On the Global Distribution, Seasonality, and Budget of Atmospheric Carbonyl Sulfide (COS) and some Similarities to CO<sub>2</sub>." *Journal of Geophysical Research-Atmospheres* 112, no. D9: 1–15. <https://doi.org/10.1029/2006JD007665>.

Nagori, J., N. Nechita-Bândă, S. O. Danielache, M. Shinkai, T. Röckmann, and M. Krol. 2022. "Modelling the Atmospheric 34S-Sulfur Budget in a Column Model under Volcanically Quiescent Conditions." *Atmospheric Chemistry and Physics Discussions*. Preprint, <https://doi.org/10.5194/acp-2022-68>.

Oduro, H., A. Kamyshny Jr., A. L. Zerkle, Y. Li, and J. Farquhar. 2013. "Quadruple Sulfur Isotope Constraints on the Origin and Cycling of Volatile Organic Sulfur Compounds in a Stratified Sulfidic Lake." *Geochimica et*

*Cosmochimica Acta* 120: 251–262. <https://doi.org/10.1016/j.gca.2013.06.039>.

Oduro, H., K. L. Van Alstyne, and J. Farquhar. 2012. “Sulfur Isotope Variability of Oceanic DMSP Generation and Its Contributions to Marine Biogenic Sulfur Emissions.” *Proceedings of the National Academy of Sciences* 109, no. 23: 9012–9016. <https://doi.org/10.1073/pnas.1117691109>.

Osorio-Rodriguez, D., M. Razo-Mejia, N. F. Dalleska, A. L. Sessions, V. J. Orphan, and J. F. Adkins. 2021. “Sulfur Isotope Fractionations Constrain the Biological Cycling of Dimethylsulfoniopropionate in the Upper Ocean.” *Limnology and Oceanography* 66, no. 10: 3607–3618. <https://doi.org/10.1002/lno.11901>.

Peterson, B. J., R. W. Howarth, and R. H. Garritt. 1985. “Multiple Stable Isotopes Used to Trace the Flow of Organic Matter in Estuarine Food Webs.” *Science* 227, no. 4692: 1361–1363. <https://doi.org/10.1126/science.227.4692.1361>.

Phillips, A. A., M. E. White, M. Seidel, et al. 2022. “Novel Sulfur Isotope Analyses Constrain Sulfurized Porewater Fluxes as a Minor Component of Marine Dissolved Organic Matter.” *Proceedings of the National Academy of Sciences* 119, no. 41: e2209152119. <https://doi.org/10.1073/pnas.2209152119>.

Pos, W. H., D. D. Riemer, and R. G. Zika. 1998. “Carbonyl Sulfide (OCS) and Carbon Monoxide (CO) in Natural Waters: Evidence of a Coupled Production Pathway.” *Marine Chemistry* 62, no. 1–2: 89–101.

Radford-Knery, J., and G. A. Cutter. 1994. “Biogeochemistry of Dissolved Hydrogen Sulfide Species and Carbonyl Sulfide in the Western North Atlantic Ocean.” *Geochimica et Cosmochimica Acta* 58, no. 24: 5421–5431. [https://doi.org/10.1016/0016-7037\(94\)90239-9](https://doi.org/10.1016/0016-7037(94)90239-9).

Said-Ahmad, W., and A. Amrani. 2013. “A Sensitive Method for the Sulfur Isotope Analysis of Dimethyl Sulfide and Dimethylsulfoniopropionate in Seawater.” *Rapid Communications in Mass Spectrometry* 27, no. 24: 2789–2796. <https://doi.org/10.1002/rcm.6751>.

Said-Ahmad, W., K. Wong, M. Mcnall, et al. 2017. “Compound-Specific Sulfur Isotope Analysis of Petroleum Gases.” *Analytical Chemistry* 89, no. 5: 3199–3207. <https://doi.org/10.1021/acs.analchem.6b05131>.

Sander, S., R. Friedl, D. Golden, et al. 2006. “Chemical Kinetics and Photochemical Data for Use in Atmospheric Studies Evaluation Number 15 Report.” NASA Technical Report Server. <https://ntrs.nasa.gov/citations/20090033862>.

Sela-Adler, M., W. Said-Ahmad, O. Sivan, W. Eckert, R. P. Kiene, and A. Amrani. 2016. “Isotopic Evidence for the Origin of Dimethylsulfide and Dimethylsulfoniopropionate-Like Compounds in a Warm, Monomictic Freshwater Lake.” *Environmental Chemistry* 13, no. 2: 340–351. <https://doi.org/10.1071/EN15042>.

Ulshöfer, V. S., G. Uher, and M. O. Andreae. 1995. “Evidence for a Winter Sink of Atmospheric Carbonyl Sulfide in the Northeast Atlantic Ocean.” *Geophysical Research Letters* 22, no. 19: 2601–2604. <https://doi.org/10.1029/95GL02656>.

Von Hobe, M., G. A. Cutter, A. J. Kettle, and M. O. Andreae. 2001. “Dark Production: A Significant Source of Oceanic COS.” *Journal of Geophysical Research. Oceans* 106, no. C12: 31217–31226. <https://doi.org/10.1029/2000JC000567>.

Von Hobe, M., R. Najjar, A. Kettle, and M. Andreae. 2003. “Photochemical and Physical Modeling of Carbonyl Sulfide in the Ocean.” *Journal of Geophysical Research. Oceans* 108, no. C7: 3229. <https://doi.org/10.1029/2000JC000712>.

Von Hobe, M., D. Taraborrelli, S. Alber, et al. 2023. “Measurement Report: Carbonyl Sulfide Production During Dimethyl Sulfide Oxidation in the Atmospheric Simulation Chamber SAPHIR.” *Atmospheric Chemistry and Physics* 23, no. 18: 10609–10623. <https://doi.org/10.5194/acp-23-10609-2023>.

Wehr, R., R. Commane, J. W. Munger, et al. 2017. “Dynamics of Canopy Stomatal Conductance, Transpiration, and Evaporation in a Temperate Deciduous Forest, Validated by Carbonyl Sulfide Uptake.” *Biogeosciences* 14, no. 2: 389–401. <https://doi.org/10.5194/bg-14-389-2017>.

Whelan, M., S. Lennartz, T. Gimeno, et al. 2018. “Reviews and Syntheses: Carbonyl Sulfide as a Multi-Scale Tracer for Carbon and Water Cycles.” *Biogeosciences* 15, no. 12: 3625–3657. <https://doi.org/10.5194/bg-15-3625-2018>.

Wortmann, U. G., S. M. Bernasconi, and M. E. Böttcher. 2001. “Hypersulfidic Deep Biosphere Indicates Extreme Sulfur Isotope Fractionation During Single-Step Microbial Sulfate Reduction.” *Geology* 29, no. 7: 647–650. [https://doi.org/10.1130/0091-7613\(2001\)029<0647:HDBIES>2.0.CO;2](https://doi.org/10.1130/0091-7613(2001)029<0647:HDBIES>2.0.CO;2).

Xie, H., R. M. Moore, and W. L. Miller. 1998. “Photochemical Production of Carbon Disulphide in Seawater.” *Journal of Geophysical Research: Oceans* 103, no. C3: 5635–5644. <https://doi.org/10.1029/97JC02885>.

Xu, F., H.-H. Zhang, X.-S. Zhong, et al. 2024. “Rapid Cycling and Emission of Volatile Sulfur Compounds in the Eastern Indian Ocean: Impact of Runoff Inputs and Implications for Balancing Atmospheric Carbonyl Sulfide Budget.” *Water Research* 267: 122475. <https://doi.org/10.1016/j.watres.2024.122475>.

Zhang, L., R. S. Walsh, and G. A. Cutter. 1998. “Estuarine Cycling of Carbonyl Sulfide: Production and Sea–Air Flux.” *Marine Chemistry* 61, no. 3–4: 127–142. [https://doi.org/10.1016/S0304-4203\(98\)00015-2](https://doi.org/10.1016/S0304-4203(98)00015-2).

## Supporting Information

Additional Supporting Information may be found in the online version of this article.

Submitted 02 April 2025

Revised 24 July 2025

Accepted 17 August 2025